

Parametric Analysis and Design Guidelines for a Quadruped Bounding Robot

Panagiotis Chatzakos and Evangelos Papadopoulos

Department of Mechanical Engineering, National Technical University of Athens, Athens, Greece

Abstract. - This paper attempts to set the basis for a systematic approach in designing legged robots. A dynamically stable quadruped robot running in the sagittal plane with a bounding gait is used, and a non-dimensional criterion that is based on the robot's forward speed and the required power to sustain a passive motion, is introduced. Dimensionless robot parameters ratios and desired motion variables are inputs to an optimization scheme that takes into consideration findings from experimental biology and environment specifications. Basic design guidelines, which derive from simulation results, are provided.

I. INTRODUCTION

A number of quadruped robots, capable of dynamically stable running, have been built, [1], [2], [3] and [4]. Their designers aim at operating them outside the laboratory in order to overcome the limitations of traditional wheeled and tracked vehicles. Despite the large number of publications on quadrupedal robot design, it is not evident that there is a *systematic methodology* behind the development of these robots. At best, biological data has been used to aid selection of the basic robot parameters, such as leg stiffness and hip height.

Our work is motivated by the need to have a *design tool* that would help the legged robot designer to choose among all the alternatives in terms of motion variables, system parameters, technology aspects, etc., so as to build the optimal quadruped robot depending on environment specifications. In this paper, we aim at setting the basis for such a *systematic methodology*, by guiding the designer to build a quadruped bounding robot that would minimize the power required to move along a passive trajectory for a given, normalized, speed.

In our analysis, we choose the bounding gait mainly for two reasons. To date, Raibert's quadruped is the fastest four-legged running machine built, capable of bounding at 2.9 m/s, [4], but this machine has not surpass biologists' predicted energy-saving galloping speed, [5]. Although bounding is found mainly in small, noncursorial animals, cursors may occasionally use it for locomotion over difficult terrain and for moderate-speed running, [6].

Based on the fact that simplified models, [7], and passive dynamics, [3], have been already proved to be helpful in designing controllers that result in considerable energy savings, [8], we use an *unactuated* and *conservative* model, which encodes the target behavior of the system and reveals intrinsic system properties and aspects of quadrupedal bounding that are anticipated to be used as a tool for the *optimal design* of legged robots. To broaden our analysis and reveal the effect of *scaling* in choosing the optimal robot's parameters based on the proposed di-

mensionless energy criterion, motion variables and ground parameters, *dimensional analysis* is employed to a simple model of quadrupedal running in the sagittal plane.

The rest of the paper is organized as follows. A simple template that is used for quadrupedal running in plane is described in Section II. Section III presents a dimensional analysis of the system, while in Section IV the unactuated and conservative model of the system is discussed. The proposed energy criterion is introduced in Section V and results along with design guidelines follow in Section VI.

II. SYSTEM MODELING

The complexity of four legged animals and robots can be reduced to relatively simple models, that can then be used to analyze system's behavior, by taking into account *synergies*, that is parts that work together in combined action or operation, and *symmetries*, that is the correspondence of parts on opposite sides of a plane through body, [7]. Such a simple model, which is commonly used to analyze the basic qualitative properties of quadrupedal running in the sagittal plane, is shown in Figure 1, while its associated parameters are given in Table 1.

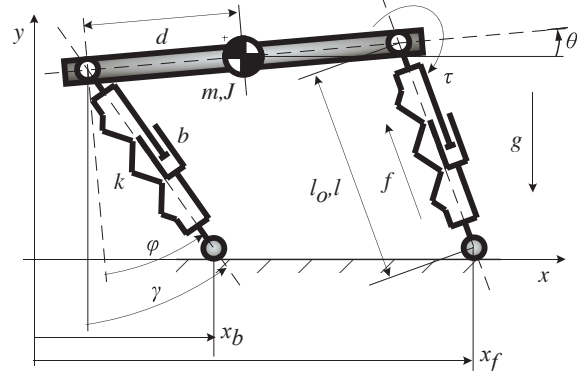


Figure 1. Parameters of the template for quadrupedal bounding in plane.

TABLE I. VARIABLES AND INDICES USED

x	COM horizontal pos.	h_{apex}	flight apex position
y	COM vertical pos.	g	acceleration of gravity
θ	body pitch angle	m	body mass
γ	leg absolute angle	J	body inertia
ϕ	leg relative angle	d	hip joint to COM distance
x_{br}	back toe horizontal pos.	f	as index: front leg
x_{fr}	front toe horizontal pos.	b	as index: back leg
l	leg length	g	as index: ground variable
l_o	leg rest length	e	specific resistance
τ	torque delivered at hip	j	dimensionless inertia
f	axial force at leg	r	relative leg stiffness
f_c	coulomb friction	p	dimensionless hip separation
b	damping coefficient	Fr	Froude number
T	cycle duration	s	time scale
T_s	stance duration	*	as superscript: dimensionless

This planar model, which represents the lateral half of a quadruped, consists of a rigid body and two springy mas-

This work is co-funded by public (European Social Fund 75% and General Secretariat for Research and Technology 25%) and private funds (Zenon SA), within measure 8.3 of Op. Pr. Comp., 3rd CSP-PENED'03.

sless legs, one attached to the body at the front and the other attached at the rear. Actuators control the orientation of each leg with respect to the body and the axial thrust delivered by each leg. Each modeled leg represents the back or the front *leg pair*, in which the two back or front legs are always in phase and it is called the *virtual leg*, [4]. Each virtual leg has twice the stiffness of the robot leg and includes friction modeling, as the sum of Coulomb and viscous friction. The torque delivered at the hip of each robot leg and the force delivered along each robot leg is equal to half the corresponding ones at the virtual leg.

System dynamics are derived using a *Lagrangian* formulation, with generalized coordinates *Cartesian* variables describing the center of mass (COM) position and the main body's attitude. During flight, the robot is under the influence of gravity only. Throughout the stance phase, the robot's toes are fixed on the ground, and act as lossless pivot joints. The dynamics for any phase may be derived from that of the double stance, by removing appropriate terms. Hence, only the double stance dynamics is given, as a set of differential and algebraic equations,

$$m\ddot{x} = -\left(f_b + k(l_o - l_b) - f_{fr,b}\right)\sin\gamma_b - \tau_b \cos\gamma_b/l_b - \left(f_f + k(l_o - l_f) - f_{fr,f}\right)\sin\gamma_f - \tau_f \cos\gamma_f/l_f \quad (1)$$

$$m\ddot{y} = \left(f_b + k(l_o - l_b) - f_{fr,b}\right)\cos\gamma_b - \tau_b \sin\gamma_b/l_b + \left(f_f + k(l_o - l_f) - f_{fr,f}\right)\cos\gamma_f - \tau_f \sin\gamma_f/l_f - mg \quad (2)$$

$$J\ddot{\theta} = \tau_b - d\left(f_b + k(l_o - l_b) - f_{fr,b}\right)\cos(\gamma_b - \theta) + \tau_f + d\left(f_f + k(l_o - l_f) - f_{fr,f}\right)\cos(\gamma_f - \theta) + d\tau_b \sin(\gamma_b - \theta)/l_b - d\tau_f \sin(\gamma_f - \theta)/l_f \quad (3)$$

where,

$$\begin{cases} \gamma_b = \text{Atan2}(y - d \sin \theta, x_{bt} + d \cos \theta - x) \\ \gamma_f = \text{Atan2}(y + d \sin \theta, x_{ft} - d \cos \theta - x) \end{cases} \quad (4)$$

$$l_b = \sqrt{(x_{bt} - x + d \cos \theta)^2 + (d \sin \theta - y)^2} \quad (5)$$

$$l_f = \sqrt{(x_{ft} - x - d \cos \theta)^2 + (d \sin \theta + y)^2} \quad (6)$$

$$f_{fr,i} = f_c \text{sign}(\dot{l}_i) + b \dot{l}_i, \quad i = b, f. \quad (6)$$

III. DIMENSIONAL ANALYSIS

Dimensional analysis can be applied to all quantitative models and offers an efficient way to display complex data sets. Usually, it makes the subsequent analysis much more useful because the physical model, as first written, is rather general. The premise of dimensional analysis is that complete equations can be written in a form that is independent of the choice of units. The consequence is that the variables that appear in a complete equation must appear in combinations that are dimensionless. Such dimensionless variables are introduced as follows,

$$t^* = t/s \quad (7)$$

$$x^* = x/l_o, \quad \dot{x}^* = s \dot{x}/l_o, \quad \ddot{x}^* = s^2 \ddot{x}/l_o \quad (8)$$

$$y^* = y/l_o, \quad \dot{y}^* = s \dot{y}/l_o, \quad \ddot{y}^* = s^2 \ddot{y}/l_o \quad (9)$$

$$\theta^* = \theta, \quad \dot{\theta}^* = s \dot{\theta}, \quad \ddot{\theta}^* = s^2 \ddot{\theta} \quad (10)$$

where s is the time scale of the system and derives from the fact that the variables that appear in a complete equation must appear in combinations that are dimensionless.

By substituting (7) – (10) to the equations of motion, given by (1) – (6), one gets a dimensionless description of the system. The resulting motion of the COM can be characterized by two distinct time scales s that represent the inverse of natural frequency of the vertical oscillation,

$$s^2 k/m = 1 \Rightarrow s = \sqrt{m/k} \quad (11)$$

and the horizontal motion, respectively,

$$s^2 g/l_o = 1 \Rightarrow s = \sqrt{l_o/g}. \quad (12)$$

Selection of the latter as the time scale of the system, results to a number of dimensionless parameter groups, which are widely used by experimental biologists. These include (a) the *Froude number* Fr , [1], defined as

$$Fr = v/\sqrt{g l_o} \quad (13)$$

where v is the robot forward speed, (b) the *dimensionless inertia* j , i.e. the robot's body inertia normalized to md^2 ,

$$j = J/md^2 \quad (14)$$

and, (c) the leg *relative stiffness* r , [11], that is defined as

$$r = k l_o/mg. \quad (15)$$

For offering this advantage, and because we are primarily interested in the forward motion aspects, the time scale in (12) is selected to set the equations of motion dimensionless. The following dimensionless parameters are also introduced. Firstly, the ratio of half of hip separation to leg rest length p , defined as,

$$p = d/l_o \quad (16)$$

and secondly, the dimensionless viscous friction coefficient b^* , defined as

$$b^* = b/m\sqrt{l_o/g} \text{ or } b^* = 2\zeta\sqrt{r} \quad (17)$$

where ζ is the damping ratio. Force and torque variables are normalized as

$$f_i^* = f_i/mg, \quad i = b, f, c \text{ and } \tau_i^* = \tau_i/mg l_o, \quad i = b, f \quad (18)$$

The desired dimensionless description of the system results from substituting (7) – (10), (12) and (14) – (18) to (1) – (6) and it is presented next for the double stance

$$\ddot{x}^* = \left(f_{fr,b}^* - f_b^* - r(1-l_b^*)\right)\sin\gamma_b^* - \tau_b^*/l_b^* \cos\gamma_b^* + \left(f_{fr,f}^* - f_f^* - r(1-l_f^*)\right)\sin\gamma_f^* - \tau_f^*/l_f^* \cos\gamma_f^* \quad (19)$$

$$\ddot{y}^* = \left(f_b^* + r(1-l_b^*) - f_{fr,b}^*\right)\cos\gamma_b^* - \tau_b^*/l_b^* \sin\gamma_b^* + \left(f_f^* + r(1-l_f^*) - f_{fr,f}^*\right)\cos\gamma_f^* - \tau_f^*/l_f^* \sin\gamma_f^* - 1 \quad (20)$$

$$p j \ddot{\theta}^* = -\left(f_b^* + r(1-l_b^*) - f_{fr,b}^*\right)\cos(\gamma_b^* - \theta^*) + \left(f_f^* + r(1-l_f^*) - f_{fr,f}^*\right)\cos(\gamma_f^* - \theta^*) + \tau_b^*/p + \tau_f^*/p + \tau_b^* \sin(\gamma_b^* - \theta^*)/l_b^* - \tau_f^* \sin(\gamma_f^* - \theta^*)/l_f^* \quad (21)$$

where,

$$\begin{cases} \gamma_b^* = \text{Atan2}(y^* - p \sin \theta^*, x_{bt}^* + p \cos \theta^* - x^*) \\ \gamma_f^* = \text{Atan2}(y^* + p \sin \theta^*, x_{ft}^* - p \cos \theta^* - x^*) \end{cases} \quad (22)$$

$$l_b^* = \sqrt{(x_{bt}^* - x^* + p \cos \theta^*)^2 + (p \sin \theta^* - y^*)^2} \quad (23)$$

$$l_f^* = \sqrt{(x_{ft}^* - x^* - p \cos \theta^*)^2 + (p \sin \theta^* + y^*)^2} \quad (23)$$

$$f_{fr,i}^* = f_c^* \text{sign}(\dot{l}_i^*) + b^* \dot{l}_i^*, \quad i = b, f. \quad (24)$$

Dynamically similar motions require that the dimensionless parameters in (14) – (16) are equal for motions with the same and the same dimensionless motion variables, e.g., flight apex, body pitch angle and pitch rate.

IV. PASSIVE DYNAMICS

It is generally accepted that bounding is essentially a natural mode of the system, and that only minor control and energy efforts are required to maintain running. Practically, this motivated us to study the *passive dynamics* of the system. If the system stays close to its passive behavior, then the actuators have less work to do to maintain the motion and energy efficiency is improved. Energy savings of 93% are reported, using passive running, in [8].

It is important to note that in this paper we use a *conservative model* that encodes the target behavior of the system and reveals intrinsic system properties and aspects of quadrupedal bounding that may be used as guidelines for the optimal design of legged robots. The passive and conservative model of our analysis is derived from (19) – (21) by eliminating actuation and energy dissipation terms and is given here for completeness,

$$\ddot{x}^* = -r(1-l_b^*)\sin\gamma_b^* - r(1-l_f^*)\sin\gamma_f^* \quad (25)$$

$$\dot{y}^* = r(1-l_b^*)\cos\gamma_b^* + r(1-l_f^*)\cos\gamma_f^* - 1 \quad (26)$$

$$\ddot{\theta} = r\left((1-l_f^*)\cos\phi_f^* - (1-l_b^*)\cos\phi_b^*\right)/p \quad (27)$$

$$\begin{aligned} \gamma_b^* &= \text{Atan2}\left(y^* - p\sin\theta^*, x_{bt}^* + p\cos\theta^* - x^*\right) \\ \gamma_f^* &= \text{Atan2}\left(y^* + p\sin\theta^*, x_{ft}^* - p\cos\theta^* - x^*\right) \end{aligned} \quad (28)$$

$$\begin{aligned} \gamma_b^* &= \theta^* + \phi_b^* \\ \gamma_f^* &= \theta^* + \phi_f^* \end{aligned} \quad (29)$$

$$\begin{aligned} l_b^* &= \sqrt{\left(x_{bt}^* - x^* + p\cos\theta^*\right)^2 + \left(p\sin\theta^* - y^*\right)^2} \\ l_f^* &= \sqrt{\left(x_{ft}^* - x^* - p\cos\theta^*\right)^2 + \left(p\sin\theta^* + y^*\right)^2} \end{aligned} \quad (30)$$

In order to evaluate the performance of the above model, we focus on system *periodic steady state trajectories*, which are trajectories that repeat themselves after one cycle of locomotion. Following a similar procedure as in [3], we employ a Poincaré Map technique to formulate these trajectories. The return map maps the state at a particular event during locomotion to the same event at the next cycle. The *apex height* is chosen to be this particular event, because the vertical velocity is always zero there. Furthermore, the forward distance has no influence in the next cycle of locomotion. Thus, the state vector \mathbf{x}^* at apex height consists only of apex height, body pitch angle, forward speed and body pitch rate,

$$\mathbf{x}^* = \begin{bmatrix} y^* & \theta^* & \dot{x}^* & \dot{\theta}^* \end{bmatrix}. \quad (31)$$

The vector state at apex height constitutes the initial conditions for the cycle. Based on these, double flight equations (derived from (25) – (27) by removing terms not permanent to the phase) are integrated, until one of the touchdown events occurs, e.g., back leg or front leg stance. This event triggers the next phase, whose dynamics are integrated using as initial conditions the final conditions of the previous state. Depending on system configuration, the next phase could be either double flight, i.e., bounding without double stance, or double stance.

The limiting case of bounding with zero body pitch rate results to pronging, and the touchdown event is then the double stance followed by the double flight.

Successive forward integration of the dynamic equations of all the phases yields the state vector of the next stride at apex height, which is the value of the Poincaré return map \mathbf{F} . If the state vector at the new apex height is identical to the initial one, the cycle is repetitive and it yields a *fixed point*. Mathematically, this is given as

$$\mathbf{x}_{n+1}^* = \mathbf{F}\left(\mathbf{x}_n^*\right). \quad (32)$$

Existence of such fixed points seems to be the rule, rather than the exception.

In order to determine the conditions required to result in steady state cyclic motions, we resort to numerical evaluation of the return map using a Newton-Raphson method. By employing this method, a large number of fixed points can be found for different initial conditions and different touchdown angles, which although they are not part of the state vector and do not participate in the dynamics, they directly affect the value of the return map as they determine touchdown and liftoff events and impose constraints on the motion of robot during back leg, front leg and double stance phases.

Variant combinations of robot's dimensionless parameters, as defined in (14) – (16), also result to different fixed points. These design parameters vary between their extreme values found either in experimental biology references, [12] and [13], or imposed by common sense. Particularly, they range as follows

$$j = 0.6 - 1.2, r = 10 - 30, p = 0.3 - 1.0 \quad (33)$$

V. ENERGETIC COST OF LOCOMOTION

Following the previous assumptions, the robot executes a passive motion according to the sets of initial conditions found by employing the above-mentioned method that is in favor of its *natural dynamics*. In this case, no energy is lost or added to the system. This may sound unrealistic, but if one uses actuators *just* to compensate for the lost energy, and initial conditions that yield a passive trajectory, then the robot will execute an active gait, very close to the passive gait and the system can be then studied as in the lossless case, which is described by (25) – (30).

The only energy required then to sustain the motion is the amount dissipated over one stride, E , which is the sum of the mechanical energy dissipated due to friction at legs E_m , the kinetic energy lost in ground damping and compression at touchdown E_g and the electrical losses due to ohmic resistances at the motors E_{el} ,

$$E = E_m + E_g + E_{el}. \quad (34)$$

At length, the dimensionless mechanical energy losses due to leg friction are found using (35) to be

$$E_m^* = f_c^* T_s + b^* \left(\int_0^{T_{sb}} l_b^{*2} dt^* + \int_0^{T_{sf}} l_f^{*2} dt^* \right) \quad (35)$$

In addition to friction losses, energy losses due to interaction of robot's legs with the ground exist. Particularly, the running robot dissipates some of its kinetic energy in ground damping and ground compression at touchdown. Ground spring and damper influence the robot only when the feet are in contact with the ground, i.e., vertical velocity is negative, while the acting direction of ground spring-damper system is along the direction of robot's interacting leg. Each time a foot touches the ground, the rest position

of the ground spring is reset to the point at which the foot first touches. The coefficient of friction between each foot and ground is assumed to be so large that slipping never occurs. Finally, for a wide yet reasonable range of damping and stiffness coefficients, the ground displacement (deformation) is negligible compared to leg length, and the integrated robot and ground motion equations can be approximated by (25) – (30) and (36)

$$b_g^* l_{g,i}^* + r_g l_{g,i}^* = r (l_i^* - 1), \quad i = b, f, \quad (36)$$

while the ratio of dimensionless ground damping to spring coefficient is the dimensionless ground time constant

$$\tau_g^* = b_g^* / r_g \quad (37)$$

To this end, the dimensionless ground energy losses due to ground damping and ground permanent deformation for each leg are found using (38) to be

$$E_{g,i}^* = \int_0^{T_{s,i}} (b_g^* l_{g,i}^* + r_g l_{g,i}^*) l_{g,i}^* dt^*, \quad i = b, f. \quad (38)$$

Electrical losses due to motor ohmic resistance also exist, but are not considered here due to lack of space. However, based on preliminary simulations, although they affect the amount of dissipated energy, they do not change the optimal set of robot's parameters as they are proportional to the square of the mechanical and ground losses sum. Detailed results on their contribution will be reported in an upcoming paper.

In our analysis, distance covered is the major consideration. Therefore, as our criterion, we consider the energy cost for moving a unit distance. Since the rate of dissipated energy per unit time is the required power P to sustain the passive motion over one cycle, and since the rate of distance covered per unit time is the forward speed of locomotion v , and if the power cost for moving with unit speed is normalized to a robot's weight mg , then a dimensionless criterion, called *specific resistance*, [14], is defined,

$$e = P / (mgv). \quad (39)$$

In such a case, robot parameters and/ or motion variables should be chosen so that the criterion in (39) is minimized.

It is has been well shown that passive running is the most efficient type. Nevertheless, depending on the initial conditions, the characteristics of a passive gait, such as the stance duration and the energy dissipated, will vary. To analyze this effect in the dimensionless framework, we define a variation of e , using dimensionless parameters, as

$$e^* = P^* / v^* = E^* / (T^* Fr / 2p) \quad (40)$$

where P^* is the dimensionless required mean power, and v^* the dimensionless forward speed. Our work has shown that e^* varies for different gaits, and that the differences are considerable. Hence, it is necessary to evaluate the effect of each dimensionless parameter and/or of their ratios to the e^* and identify the set of parameters, for which the criterion in (40) is least.

If an optimal set of robot parameters has been chosen for a given set of initial conditions and ground properties, and if say the ground properties change, then these parameters may require adjustment to maintain optimality. This is consistent with the policy chosen by animals, which they will adjust leg stiffness for running economically on different ground surfaces or at higher speeds, [9]. Therefore, a range of ground stiffnesses and damping properties are going to be used so as to determine their ef-

fect on the performance of the system, i.e., on the value of criterion in (40).

VI. RESULTS, DISCUSSION AND DESIGN GUIDELINES

In this section, the results of our analysis are presented and design guidelines are proposed. The results are obtained by simulation and for a range of robot/ environment parameters. In each figure, the *cost of locomotion*, as defined in (40), is plotted versus two dimensionless robot parameters or motion variables. The *hollow stars* denote the optimal value of the variable that lies in the horizontal axis for a given value of the variable in the vertical axis, while the *filled star* represents the global minimum of the criterion, i.e. the optimal set of robot parameters or motion variables, which yields a *design guideline* for a given robot, known ground specifications and a particular trajectory. Each time the “non-participating” parameters are fairly changed so as to show that our results are not limited to a certain range of values.

The profound effect of *relative stiffness* and *pitch rate* on dimensionless specific resistance for a given set of system parameters and motion variables is shown in Figure 2. As shown in this figure, the effect of relative stiffness on mechanical (left) and ground (middle) specific resistance is competitive. Mechanical specific resistance is minimized for the larger relative stiffness, while ground specific resistance takes its lowest value for the smaller one. For example, usage of soft springs, which result to relatively smaller relative stiffness, will cause more leg compression compared to harder ones causing excessive energy dissipation due to friction. But, the resulting forces that interact with the ground will be much smaller than the ones produced by harder leg springs resulting to minimal energy dissipation due to ground damping and compression. Still, this competitive effect ensures the existence of an optimal relative stiffness that minimizes the cost of locomotion, (40), as illustrated in Figure 2 (right).

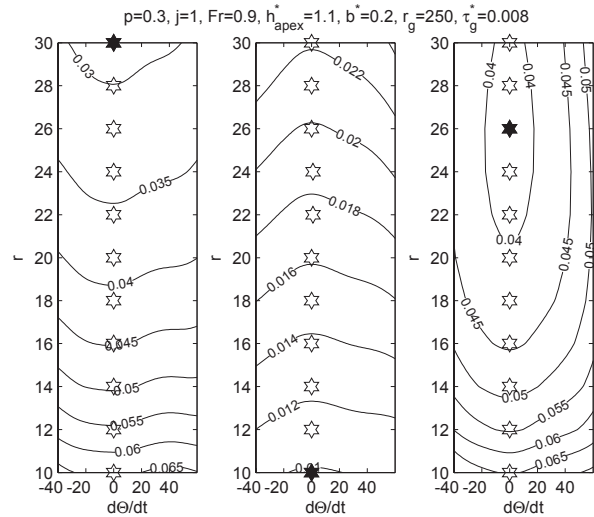


Figure 2. The effect of relative stiffness and pitch rate on mechanical (right), ground (middle) and overall (right) specific resistance.

In Figure 2, it is also evident that mechanical (left) and ground (middle) specific resistance is a convex and concave function of pitch rate, respectively, for given relative stiffness. This leads to the conclusion that the optimal pitch rate will be zero, as shown in Figure 2 (right). Thus, the most economical type of bounding is for the limiting case where the back and front *leg pairs* are in phase, i.e., pronging.

However, the optimal value of leg stiffness should be adjusted to ground stiffness for the robot to move in the most economically way all the time. This is concluded from Figure 3, where the effect of leg and ground relative stiffness on overall specific resistance is plotted for zero pitch rate, i.e., pronking. The relationship between them is linear, implying that one should not search for an optimal value of relative stiffness, but rather one should determine the optimal leg to ground stiffness *ratio*. This is also supported by experimental biology findings, [9], as animals adjust their leg stiffness for running economically on different ground surfaces.

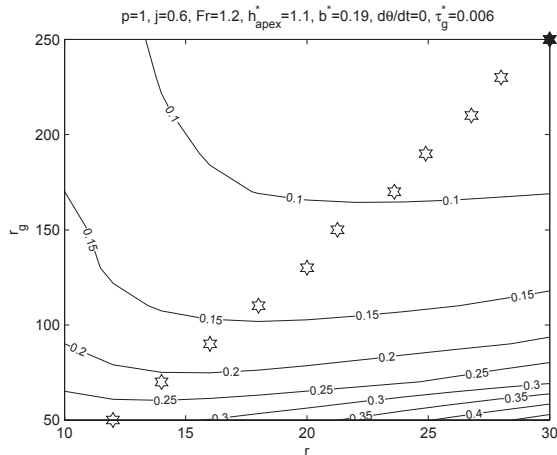


Figure 3. The effect of leg and ground relative stiffness on overall specific resistance.

Although not shown here due to lack of space, the shape of the *geometric locus*, along which the optimal set of leg and ground stiffness is moving, heavily depends on the dimensional viscous friction coefficient. For ground losses are independent of viscous friction, while mechanical power losses are proportional to viscous friction coefficient, the optimal leg to ground stiffness ratio set is moving to the right or left when b^* increases or decreases, respectively. Yet, for a given robot, known ground and particular motion variables the optimal leg relative stiffness can be estimated with the aid of Figure 2 and Figure 3.

Additionally, for every value of leg relative stiffness an optimal dimensionless forward speed exists. This is indicated in Figure 4, where the effect of *relative stiffness* and *Froude number* on overall specific resistance is drawn.

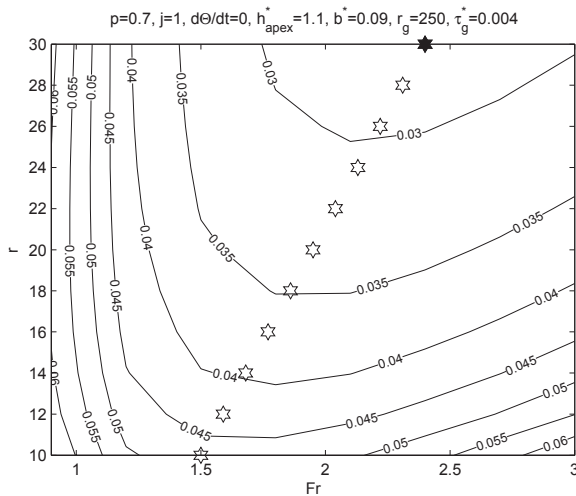


Figure 4. The effect of relative stiffness and Froude number on overall specific resistance.

Specifically, the optimal running speeds of the quadruped lie along a steep line for a wide range of relative stiffness values. This fact imposes that the robot could be designed for a *nominal forward speed*, as selected with the aid of Figure 4, and operated close to its economical function for a sufficient variation of forward speeds. One may also notice that the range of optimal forward speed is between 1.5 and 2.4. In this range lies the Froude number that corresponds to the preferred bounding speed of many quadrupeds, [1]. Outside this range, these animals prefer to walk (for slower speeds) or gallop (for higher speeds).

The existence of an optimal forward speed for given robot configuration and ground specifications is also consistent with [15]. Although a one legged robot is studied in [15], the dynamics of the *pronking* quadruped is similar to those of one-leg hopper. In the end, [15] concludes that there exists a particular passive gait, of all those possible, i.e., an optimal touchdown angle, that leads to the least dissipated energy per meter of travel. This optimal touchdown angle results to a particular (optimal) forward speed.

In Figure 5, the effect of dimensionless *hip separation* and *pitch rate* on mechanical (left), ground (middle) and overall (right) specific resistance is presented. Forward speed is *normalized* to body length, according to (40). Two are the prominent conclusions drawn from this figure. Firstly, the optimal pitch rate for a given dimensionless body length is zero. This strengthens the conclusion drawn precisely from Figure 2 (right), that *pronking* is the most economical type of bounding for a running robot in the sagittal plane. Secondly, mechanical, ground and overall specific resistance exhibit a global minimum value, which corresponds to different values of the dimensionless hip separation though.

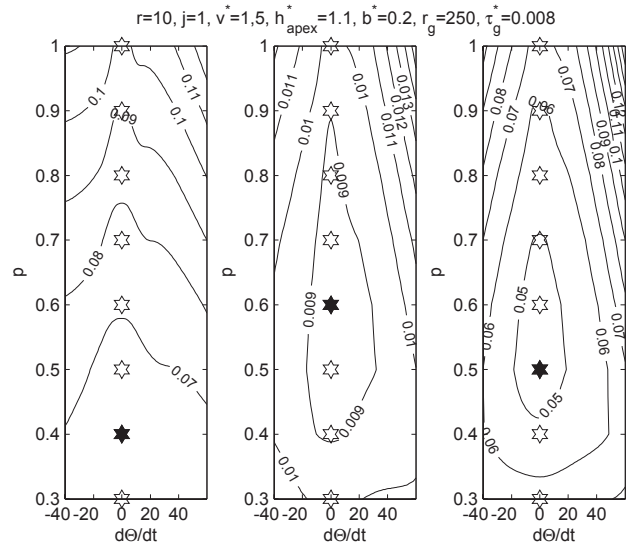


Figure 5. The effect of dimensionless body length and pitch rate on mechanical (left), ground (middle) and overall (right) specific resistance.

This optimal value of the dimensionless *hip separation* that minimizes the cost of locomotion, Figure 5 (right), depends mostly on *relative stiffness*. Actually, there exists an *optimal ratio* between the two variables, which ensures that overall specific resistance is minimal. This is justified in Figure 6, where mechanical (right), ground (middle) and overall (right) specific resistance with respect to dimensionless body length and relative stiffness is plotted. Large values of relative stiffness result to small mechanical specific resistance. Contrarily, ground specific resistance is reduced for small values of the relative stiffness.

Furthermore, for given relative stiffness, the mechanical and ground specific resistance is rather a convex and concave function of the dimensionless hip separation. All these justify the shape of the geometrical locus, Figure 6 (right), along which the optimal set of relative stiffness and hip separation, which minimizes (40), is moving. With the aid of this figure, the optimal dimensionless body length may be determined for a given robot, known ground and provided that the optimal relative stiffness has been selected with the aid of Figure 2 and Figure 3.

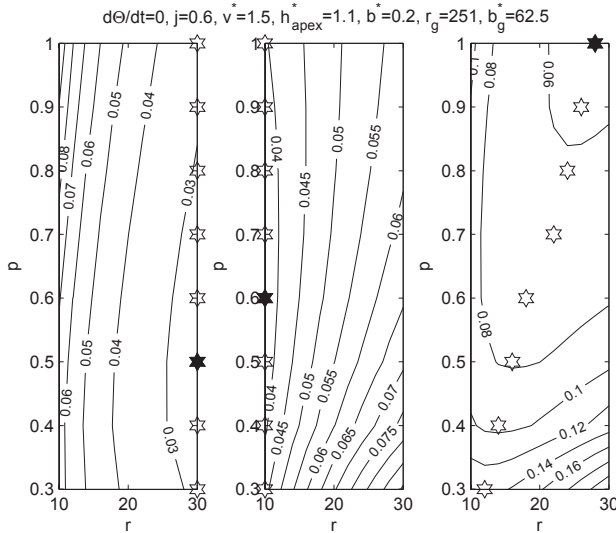


Figure 6. The effect of dimensionless stiffness and body length on mechanical (right), ground (middle) and overall (right) specific resistance.

Finally, the effect of *dimensionless inertia* and *pitch rate* on overall specific resistance is presented in Figure 7. Their effect is complex. For large, either negative or positive pitch rates, the overall specific resistance is reduced when the dimensionless inertia decreases. On the contrary, for pitch rates close to zero the overall specific resistance is almost constant up to $j=1$, while for even larger values, the overall specific resistance is reduced. Surprisingly the global minimum values are found for small pitch rates, round -7.5 and 7.5, and for the larger value of dimensionless inertia ($j=1.2$). Nevertheless, the effect of dimensionless inertia is not significant to the overall specific resistance, for small pitch rates, so perhaps other criteria should guide the designer to select its value, such as stability, control aspects and/ or design simplification.

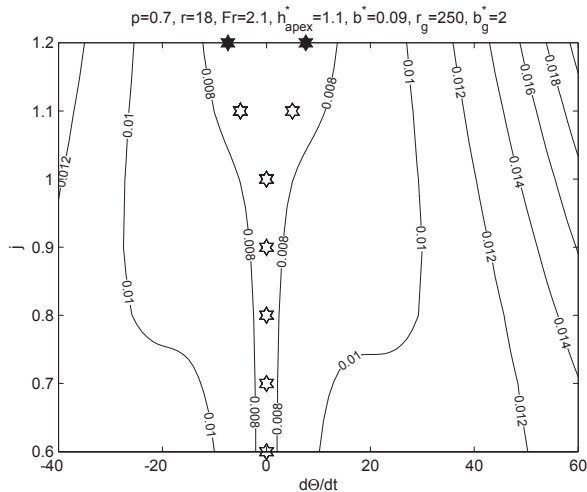


Figure 7. The effect of dimensionless inertia and pitch rate on overall specific resistance.

CONCLUSIONS

In this paper, we set the basis for a systematic approach in designing low-consumption legged robots. An unactuated and conservative model of a dynamically stable quadruped robot running in the sagittal plane with a bounding gait was parametrically analyzed, so as to reveal the effect of scaling, intrinsic system properties, and aspects of quadrupedal running. A dimensionless criterion, based on the robot forward speed and the required power for passive motion, was introduced. Taking into account ground specification, system parameters and motion variables were selected so as to minimize the cost of locomotion. The proposed approach can guide a designer to build an energy per distance optimal quadruped bounding robot by parametrically encoding its energetic behavior and following the presented methodology and guidelines.

In the future, we are planning to include electrical losses and examine the effect of ground inclines on the locomotion cost. Other gaits, different types of legs, e.g., two segment legs with compliant knees, and body asymmetry will also be investigated. The effect of scaling on self-stabilization for facilitating simple controllers is our last target. Ultimately, it is hoped that we will be able to answer the question regarding which design is "globally" optimal be having only minimal specifications.

REFERENCES

- [1] Kimura H., Sakurama K. and Akiyama S., "Dynamic Walking and Running of the Quadruped Using Neural Oscillator", *Autonomous Robots*, Vol. 7(3), 1999.
- [2] Nicol J. G. and Waldron K. J., "Biomimetic leg design for un-tethered quadruped gallop", in the Proc. Of the CLAWAR Int. Conf. on Climbing and Walking Robots, Paris, France, 2002.
- [3] Poulakakis I., Papadopoulos E. G. And Buehler M., "On the Stability of the Passive Dynamics of Quadrupedal Running with a Bounding Gait", in the Int. J. of Robotics Research, Vol. 25, 2006.
- [4] Raibert M. H., "Legged Robots that Balance", MIT Press, Cambridge MA, 1986.
- [5] Heglund N. C. and Taylor C. R., "Speed, stride frequency and energy cost per stride: How do they change with body size and gait?", in the J. of Experimental Biology, Vol. 138, 1988.
- [6] Gambaryan P. P., "How Mammals Run: Anatomical Adaptations", Wiley, New York, 1974.
- [7] Full R. J. and Koditschek D., "Templates and Anchors: Neuromechanical Hypotheses of Legged Locomotion in Land", in the J. of Experimental Biology, Vol. 202, 1999.
- [8] Ahmadi M. and Buehler M., "Stable Control of a Simulated One-Legged Running Robot with Hip and Leg Compliance", in IEEE Transactions on Robotics & Automation 13, No. 1, 1997.
- [9] Alexander R. M., "Principles of Animal Locomotion", Princeton University Press, Princeton NJ, 2003.
- [10] Murphy K. N. and Raibert M. H., "Trotting and Bounding in a Planar Two-legged Model", in 5th Symposium on Theory and Practice of Robots and Manipulators, Cambridge, MA, 1984.
- [11] Blickhan R., "The spring-mass model for running and hopping", in the J. of Biomechanics, Vol. 22, 1989.
- [12] Farley C.T., Glasheen J., and McMahon T.A., "Running Springs: Speed and Animal Size", in the J. of Experimental Biology, Vol. 185, 1993.
- [13] Herr H. M., Huang G.T. and McMahon T. A., "A model of scale effects in mammalian quadrupedal running", in the J. of Experimental Biology, Vol. 205, 2002.
- [14] Gabrielli G. and von Karman T., "What price speed? Specific power required for propulsion of vehicles", in the Mechanical Engineering, ASME, Vol. 72 (10), 1950.
- [15] Cherouvim, N. and Papadopoulos, E., "Energy Saving Passive-Dynamic Gait for a One-Legged Hopping Robot," in *Robotica*, Vol. 24, No. 4, 2006.